

Evidence for a $k^{-5/3}$ Spectrum from the EOLE Lagrangian Balloons in the Low Stratosphere

GUGLIELMO LACORATA

Institute for Atmospheric and Climate Science, CNR, Lecce, Italy

ERIK AURELL

Department of Physics, KTH Royal Institute of Technology, Stockholm, Sweden

BERNARD LEGRAS

Laboratoire de Météorologie Dynamique, Ecole Normale Supérieure, Paris, France

ANGELO VULPIANI

Department of Physics, University of Rome "La Sapienza," and INFN (UdR and SMC), Rome, Italy

(Manuscript received 10 December 2003, in final form 11 March 2004)

ABSTRACT

The EOLE experiment is revisited to study turbulent processes in the lower stratosphere circulation from a Lagrangian viewpoint and to resolve a discrepancy on the slope of the atmospheric energy spectrum between the work of Morel and Larchevêque and recent studies using aircraft data. Relative dispersion of balloon pairs is studied by calculating the finite-scale Lyapunov exponent, an exit-time-based technique that is particularly efficient in cases in which processes with different spatial scales are interfering. The main goal is to reconcile the EOLE dataset with recent studies supporting a $k^{-5/3}$ energy spectrum in the 100–1000-km range. The results also show exponential separation at smaller scales, with a characteristic time of order 1 day, and agree with the standard diffusion of about $10^7 \text{ m}^2 \text{ s}^{-1}$ at large scales. A remaining question is the origin of a $k^{-5/3}$ spectrum in the mesoscale range between 100 and 1000 km.

1. Introduction

The EOLE project (Morel and Bandeen 1973) consisted of the release of 483 constant-volume pressurized balloons, in the Southern Hemisphere midlatitudes throughout the period September 1971–March 1972, at approximately 200 hPa. The lifetime of these balloons was from a few days to about 1 yr, with an average value of about 120 days. Their motion was basically isopycnal except for small diurnal volume variations of the envelop of less than 1% and inertial oscillations of a few meters in the vertical, excited by wind shear and small-scale turbulence. The position of the balloons and meteorological parameters were periodically transmitted to satellite by the ARGOS system. The trajectories of the EOLE experiment still provide nowadays the most extensive dataset of experimental quasi-Lagrangian tracers in the atmosphere for observing the properties

of the medium to large-scale motion at the tropopause level.

Both Eulerian and Lagrangian analyses have been performed by several authors. Morel and Desbois (1974) deduced the mean circulation around 200 hPa from the balloon flights, as formed by a midlatitude zonal stream with a meridional profile characterized by a typical velocity $\sim 30 \text{ m s}^{-1}$ inside the jet, overlaid to meridional velocity field disturbances of much smaller intensity, $\sim 1 \text{ m s}^{-1}$, and to residual standing waves acting as spatial perturbations of the zonal velocity pattern, producing the typical shape of a meandering jet. These results have been largely confirmed by operational analysis since then.

Morel and Larchevêque (1974, hereafter ML) investigated the synoptic-scale turbulent properties. They measured the mean-square relative velocity and the relative diffusivity of balloon pairs, and found essentially two major regimes for Lagrangian dispersion: exponential separation for time delays less than 6 days, and standard diffusion for longer times. These authors observed that the scaling of the relative diffusivity with

Corresponding author address: Dr. Guglielmo Lacorata, CNR-ISAC sezione di Lecce, Str. Lecce-Monteroni, I-73100 Lecce, Italy.
E-mail: g.lacorata@isac.cnr.it

the separation length between two balloons agreed with a direct 2D turbulent cascade, with energy spectrum $E(k) \sim k^{-3}$, or steeper, in the range 100–1000 km, while the same could not be said for the mean-square relative velocity, which was found to be inconsistent with the relative diffusivity.

Further Eulerian analyses of large-scale velocity spectra by Desbois (1975) were compatible with the scenario proposed by Morel and Larchevêque (1974) about isotropic and homogeneous 2D turbulence with a k^{-3} energy distribution up to scales ~ 1000 km. Other results about the relative dispersion of stratospheric balloons come from the analysis of the Tropical Wind, Energy Conversion and Reference Level Experiment (TWERLE) dataset (see Er-El and Peskin 1981), where they also found exponential separation below 1000 km, even though at a different level (150 mb) and with noisier statistics with respect to the EOLE data.

Later, other authors reached for different conclusions after observing energy spectra in the low stratosphere, measured from experimental data recorded from commercial aircraft flights (Gage 1979; Lilly 1983; Nastrom and Gage 1985). Their picture suggested a 2D turbulent inverse cascade, characterized by the $E(k) \sim k^{-5/3}$ spectrum, inside the interval of scales 100–1000 km.

More recently, velocity spectra obtained from data recorded during the Measurement of Ozone from Airbus in Service Aircraft (MOZAIC) program were found in agreement with the $k^{-5/3}$ scenario (see Lindborg and Cho 2000, 2001; Cho and Lindborg 2001). These authors suggested a dynamical mechanism different from 2D inverse cascade where energy is injected in the large scales by breaking gravity waves (see Bacmeister et al. 1996 for a discussion on gravity wave spectra) and generates a chain process down to smaller scales. Their hypothesis is supported by the observation of a down-scale energy flux, whereas a 2D inverse cascade should exhibit upscale energy flux (Lindborg and Cho 2000).

We wanted to reconsider this issue by performing a new analysis of the relative dispersion properties of the EOLE balloons within the framework of a dynamical system theory. Relative dispersion properties are analyzed through the computation of the finite-scale Lyapunov exponent (FSLE; Aurell et al. 1997; Artale et al. 1997; Boffetta et al. 2000a). The FSLE is based on the growth rate statistics of the distance between trajectories at a fixed scale, and is a better tool to analyze scale-dependent properties than plain dispersion, as explained below. This new method has been already exploited for studies of relative dispersion in atmospheric and oceanic systems (Lacorata et al. 2001; Joseph and Legras 2002; Boffetta et al. 2001; LaCase and Ohlmann 2003; Gioia et al. 2004) and also in laboratory convection experiments (Boffetta et al. 2000b).

This paper is organized as follows: in section 2 we describe the FSLE methodology; section 3 contains the results obtained from our analysis of the EOLE experimental data; in section 4 we discuss the physical in-

formation that can be extracted from this paper and possible perspectives.

2. Finite-scale relative dispersion

Generally speaking, most flows exhibit different ranges of scales over which fluid motion is expected to display different characteristics: a small-scale range where the velocity variations can be considered as a smooth function of space variables, a range of intermediate lengths corresponding to the coherent structures (and/or spatial fluctuations) present in the velocity field over which velocity variations are rough but highly correlated, and a large-scale range over which spatial correlations have definitely decayed. In each of these ranges, relative dispersion between trajectories is governed by a different physical mechanism (chaos, turbulence, diffusion), which can be, in principle, identified from the observations. In fully developed three-dimensional turbulence, motion is only smooth under the Kolmogorov dissipative scale. In the free stratified atmosphere (above the planetary boundary layer), turbulence is a relatively rare event: motion is most often smooth but for some localized convective or turbulent events, associated with mesoscale systems, that mix momentum and tracers. Hence, one expects to find a smooth (chaotic) dispersion range ending at a scale characteristic of the spacing of mixing events, followed by a range covering the mesoscale to synoptic range, and finally standard diffusion at planetary scale. This view is supported by the ubiquitous observation of long-lived laminated structures in the free troposphere (Newell et al. 1999).

In order to fix some terminology, we will use both symbols R and δ to indicate the distance between balloons: the former will be considered as a quantity function of time, the latter as an argument for scale-dependent functions.

a. Diffusion and chaos

Diffusion is characterized in terms of diffusion coefficients, related to the elements of a diffusion tensor, defined as

$$D_{ij} = \lim_{t \rightarrow \infty} \frac{1}{2t} \langle [x_i(t) - \langle x_i(0) \rangle][x_j(t) - \langle x_j(0) \rangle] \rangle, \quad (2.1)$$

where $x_i(t)$ and $x_j(t)$ are the i th and j th coordinates at time t , with $i, j = 1, 2, 3$. The average operation denoted by angle brackets $\langle \rangle$ is meant to be performed over a large number of particles. The diagonal elements are just the diffusion coefficients. When the D_{ii} s are finite, then the diffusion is standard. This means that at long times, after the Lagrangian velocity correlations have decayed (Taylor 1921), the variance of the particle displacement follows the law

$$\langle \|\mathbf{x}(t) - \langle \mathbf{x}(0) \rangle\|^2 \rangle \approx 2Dt. \quad (2.2)$$

In presence of a velocity field characterized by co-

herent structures, it is more useful to observe the relative dispersion between the trajectories, rather than the absolute dispersion from the initial positions, given by (2.2), which is unavoidably dominated by the mean advection.

In the case of the EOLE experiment, where observing the expansion of balloon clusters with more than two elements is a rare event (ML), a measure of relative dispersion is given by the mean-square interparticle distance:

$$\langle R^2(t) \rangle = \langle \|\mathbf{x}^{(m)}(t) - \mathbf{x}^{(n)}(t)\|^2 \rangle, \quad (2.3)$$

averaged over all the pairs $[\mathbf{x}^{(m)}, \mathbf{x}^{(n)}]$, where m and n label all the available N trajectories. Notice that the norm in (2.2) and (2.3) must be defined accordingly to the geometry of the fluid domain; that is, in the atmosphere we use the arc distance on the great circle of the earth connecting the two points. The quantity in (2.3) can be measured for both initially close pairs, balloons released from the same place at short time delay; and so-called chance pairs, balloons initially distant, which come close to each other at a certain time and, later, spread away again (ML). Consistency of the average in Eq. (2.3) requires all the trajectory pairs to have nearly the same initial distance, a condition that strongly limits the statistics. At long times, $\langle R(t)^2 \rangle$ defined in Eq. (2.3) is expected to approach the function $4Dt$, where the 4 factor accounts for relative diffusion. When it happens that $\langle R(t)^2 \rangle \sim t^{2\nu}$ with $\nu > 1/2$ instead, the Lagrangian dispersion is considered as superdiffusion. A well-known example is the Richardson's law for the particle pair separation in 3D turbulence, for which $\nu = 3/2$ (Richardson 1926).

On the other hand, in the limit of infinitesimal trajectory perturbations, much smaller than the characteristic lengths of the system, the evolution of the particle pair separation is characterized by the Lyapunov exponent (Lichtenberg and Lieberman 1982), such that

$$\lambda = \lim_{t \rightarrow \infty} \lim_{R(0) \rightarrow 0} \frac{1}{t} \ln \frac{R(t)}{R(0)}. \quad (2.4)$$

If $\lambda > 0$, the growth is exponential and the motion is said chaotic. Chaos is a familiar manifestation of nonlinear dynamics, leading to strong stirring of trajectories (Ottino 1989). The process, for example, of repeated filamentation around the polar vortex is basically due to Hamiltonian chaos (Legras and Dritschel 1993). For finite perturbations within a smooth flow, the properties of exponential separation are observed for a finite time.

b. Finite-scale Lyapunov exponent

The idea of FSLE (Aurell et al. 1997; Artale et al. 1997) was formerly introduced in the framework of the dynamical systems theory in order to characterize the growth of noninfinitesimal perturbations (i.e., the distance between trajectories). If δ is the scale of the per-

turbation, and $\langle \tau(\delta) \rangle$ is the mean time that δ takes to grow a factor $r > 1$, then the FSLE is defined as

$$\lambda(\delta) = \frac{1}{\langle \tau(\delta) \rangle} \ln r. \quad (2.5)$$

The average operation is assumed to be performed over a large ensemble of realizations. For factors r not much larger than 1, $\lambda(\delta)$ does not depend sensitively on r . If $r = 2$, then $\langle \tau(\delta) \rangle$ is also called doubling time. Operatively, $N + 1$ scales are chosen to sample the spatial range of perturbation, $\delta_0 < \delta_1 < \dots < \delta_N$, and a growth factor r is defined such that $\delta_i = r\delta_{i-1}$ for $i = 1, N$. Let l_{\min} and l_{\max} be the smallest and the largest characteristic length of the system, respectively. If $\delta_0 \ll l_{\min}$, then the FSLE characterizes the doubling time of infinitesimal perturbation. In the opposite side of the range, if $\delta_N \gg l_{\max}$, then the FSLE follows the scaling law of diffusion $\lambda(\delta) \sim \delta^{-2}$ for $\delta \rightarrow \delta_N$, as can be deduced by noticing that the mean-square particle distance must grow linearly in time, see (2.2). In general, if the mean-square size of a tracer concentration follows the $\langle R^2 \rangle \sim t^{2\nu}$ law, the FSLE scales as $\lambda(\delta) \sim \delta^{-1/\nu}$, and vice versa. As we have seen before, for standard diffusion, $\nu = 1/2$, while for Richardson's superdiffusion, $\nu = 3/2$. The main interest of FSLE is to select processes occurring at a fixed scale. We stress that definition (2.5) differs substantially from

$$\lambda'(\delta) = \frac{1}{\langle R^2 \rangle} \left. \frac{d\langle R^2 \rangle}{dt} \right|_{\langle R^2 \rangle = \delta^2}, \quad (2.6)$$

which is a dispersion rate function of the (mean) separation between trajectories but defined through a totally different averaging procedure: $\langle R^2 \rangle$ is computed at fixed time, while $\tau(\delta)$ is computed at fixed scale. As a result, a physical situation that is well characterized in terms of FSLE, either for scaling properties or the existence of transport barriers, may be less easily characterized by studying the time growth of trajectory separation (Boffetta et al. 2000b; Joseph and Legras 2002). One reason is that $\langle R^2(t) \rangle$ depends on contribution from different regimes, as seen, for example in 3D turbulence where a dramatic dependence of $R^2(t)$ upon $R^2(0)$ is observed, even at very large Reynolds number (Fung et al. 1992).

In cases where advection is strongly anisotropic, for example, in the presence of a structure like the stratospheric jet stream, it may be useful to define the FSLE in terms of meridional (cross stream) displacement only:

$$\lambda_{\text{mer}}[\delta^{(\text{mer})}] = \frac{1}{\langle \tau[\delta^{(\text{mer})}] \rangle} \ln r, \quad (2.7)$$

where $\delta^{(\text{mer})}$ is the latitude distance (or meridian arc) between two points.

Information about the relative dispersion properties is also extracted by another fixed-scale statistic, the fi-

TABLE 1. Number of balloon pairs analyzed for each scale during the computation of the FSLE. The first column is the order of the scale $\delta_n = r^n \delta_0$, with $r = \sqrt{2}$; the second, third, fourth, and fifth columns refer to the initial thresholds $\delta_0 = 25, 50, 100,$ and 200 km, respectively.

n	25 km	50 km	100 km	200 km
0	495	1037	2025	3979
1	344	782	1670	3649
2	391	867	1806	3699
3	414	895	1855	3764
4	440	951	1877	3722
5	442	955	1892	3687
6	456	950	1857	3563
7	442	944	1829	3471
8	448	928	1749	3327
9	440	906	1703	3131
10	428	865	1617	2648
11	418	845	1511	
12	397	794	1277	
13	389	756		
14	368	642		
15	346			
16	290			

nite-scale relative velocity (FSRV), named by analogy with FSLE, which is defined as

$$\nu_2(\delta) = \langle \delta \mathbf{v}(\delta)^2 \rangle, \quad (2.8)$$

where

$$\delta \mathbf{v}(\delta)^2 = (\dot{\mathbf{x}}^{(1)} - \dot{\mathbf{x}}^{(2)})^2 \quad (2.9)$$

is the square Lagrangian velocity difference between two trajectories $\mathbf{x}^{(1)}$ and $\mathbf{x}^{(2)}$ on scale δ , that is, for $|\mathbf{x}^{(1)} - \mathbf{x}^{(2)}| = \delta$. The FSRV can be regarded as the second-order structure function of the Lagrangian velocity difference and provides a complementary analysis to the FSLE diagnostics. In particular, in the regime of Richardson's superdiffusion, the expected behavior for the FSRV is $\nu_2(\delta) \sim \delta^{2/3}$.

We report in the next section the results of our analysis.

3. Analysis of the EOLE Lagrangian data

After a preliminary data check, the number of balloons selected for the analysis has been reduced to 382. This has been obtained by discarding ambiguous identification numbers (some identification numbers have been used twice during the campaign), discarding trajectories that cross the equator and short tracks of less than 10 points.

Successive points along a balloon trajectory were mostly recorded at a time interval of 10^{-1} day (2.4 h), but the overall distribution of the raw data does not uniformly cover the time axis. Hence, each of the coordinates (longitude and latitude) of every balloon trajectory has been interpolated in time by a cubic spline scheme, with a sampling rate of 25 points per day. Because of possible data impurities, each Lagrangian velocity value is monitored at every time step (0.04 day),

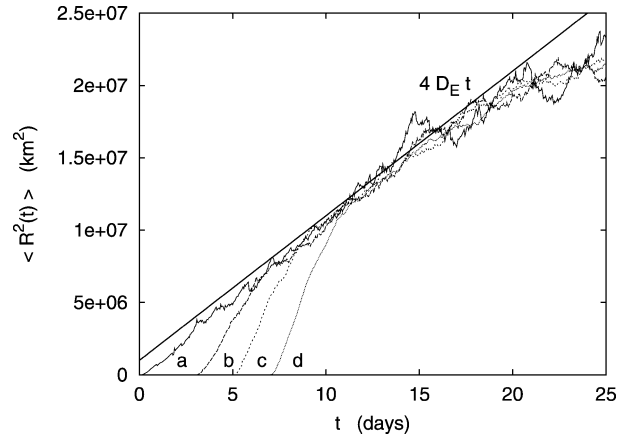


FIG. 1. Mean-square balloon separation. The four curves refer to four different initial thresholds: line a: 25, line b: 50, line c: 100, and line d: 200 km. All the curves except 25 km have been shifted in time in order to collapse together for $\langle R^2 \rangle > 10^7 \text{ km}^2$. The eddy diffusion coefficient corresponding to the indicated slope is $D_E \approx 2.9 \times 10^6 \text{ m}^2 \text{ s}^{-1}$.

and data segments with abnormally fast motions are discarded.

As pointed out by ML, a way to measure the dispersion between balloons is waiting for one of them to get close to another one, at a distance less than a threshold δ_0 , and then observing the evolution of their relative distance in time. This procedure is repeated for each balloon trajectory until the whole set of pairs is analyzed. The dataset includes original pairs of balloons that were launched within a short time interval and chance pairs of balloons meeting suddenly after a number of days. For the largest values of the threshold used in this study, the number of chance pairs largely exceeds the number of original pairs. In this way, global properties of the Lagrangian transport are extracted from the contributions of balloon pairs randomly distributed all over the domain. The number of balloon pairs and its evolution as the separation crosses the N scales defined above are described by Table 1.

In Fig. 1, four global relative dispersion curves are plotted, referring to four different initial thresholds $\delta_0 = 25, 50, 100,$ and 200 km. The statistical samples vary roughly in a proportional way with δ_0 . Relative dispersion depends sensitively, as expected, on the initial conditions; the four curves meet together for separation larger than about 2500 km and saturation begins for separation larger than 4500 km, leaving room only for a short standard diffusive regime between these two separations and over a time duration of less than 10 days. The eddy diffusion coefficient D_E , estimated by fitting the linear law $4D_E t$, results in $D_E \approx 2.9 \times 10^6 \text{ m}^2 \text{ s}^{-1}$, a value compatible with what was found by ML. The prediffusive regime is not very clear, we can say that the behavior of the balloon separation looks like a power law with exponent (changing in time) between 3 and 1.

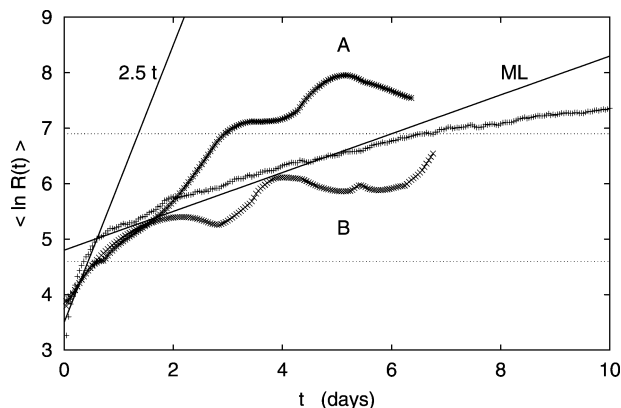


FIG. 2. Mean logarithmic growth of the balloon separation (+). The initial separation is ≤ 25 km. The two clusters A (*) and B (\times) have four balloons each and were launched with a 3-day lag in Nov 1971. The e -folding time of the exponential growth is ≈ 0.4 days. The two horizontal lines mark the 100–1000-km range (natural logarithm units). The straight line ML is the result found by Morel and Larchevêque (1974) in their Fig. 8.

We report in Fig. 2 the mean logarithmic growth of the balloon relative separation over all pairs selected by the 25-km threshold. At very short times (< 1 day) the slope corresponds to an exponential growth rate with e -folding time of ≈ 0.4 day that we consider as a rough estimate of the largest Lagrangian Lyapunov exponent (LLE). At later times, the slope gradually decreases as the separation growth tends to a power-law regime. In the same figure we also show the mean logarithmic growth of the interballoon distance computed for two four-element clusters (labeled A and B), launched with a time interval of 3 days between them. A linear behavior (exponential growth) for both clusters is observed for short intervals; we observe that the exponential regime lasts longer for the A cluster (≈ 3 days) than for the B cluster (≈ 1 days). This illustrates the fact that the duration of a dispersion regime, here the chaotic one, may exhibit large fluctuations generally due to different meteorological conditions. As a result, average time-dependent quantities, such as $\langle R^2(t) \rangle$, sample different regimes at once and are poor diagnostics of dispersion properties. Incidentally, in ML, the behavior of the relative dispersion between 100 and 1000 km is fitted by means of an exponential with characteristic e -folding time of ≈ 2.7 days (see ML, Fig. 8), which is compatible with the growth rate of Fig. 2 between the two horizontal lines marking the 100–1000-km range, if one wants to fit it with an exponential curve.

Figure 3 shows the global FSLE relatively to the same four initial thresholds used for the relative dispersion, where the amplification ratio r is set to $\sqrt{2}$. Error bars are estimated from the variance of subsamples of the FSLE, 100 pairs, relatively to the mean FSLE computed for each scale. The main result of this study is that up to about 1000 km there is evidence of Richardson's superdiffusion, compatible with a $k^{-5/3}$ spectrum, dis-

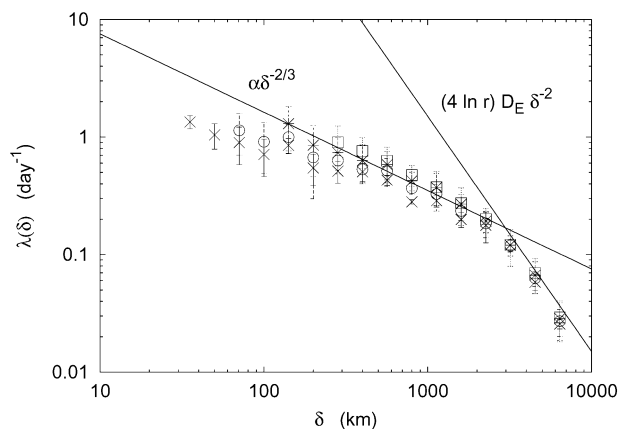


FIG. 3. FSLE of the balloon pairs [see Eq. (2.5)]. The four curves have the same initial thresholds as in Fig. 1: 25 (\times), 50 (\circ), 100 (*), and 200 (\square) km. The eddy diffusion coefficient is $D_E \approx 10^7$ m 2 s $^{-1}$. The quantity α^3 gives the order of magnitude of the relative kinetic energy growth rate (for unit mass) between balloons in the Richardson's regime $\sim \delta^{-2/3}$.

played by the behavior $\lambda(\delta) = \alpha \delta^{-2/3}$. The best fit is obtained for the initial thresholds 100 and 200 km, which encompass a much larger number of pairs than smaller thresholds (see Table 1). The quantity α^3 is physically related to the mean relative kinetic energy growth rate (for unit mass) between balloons moving apart. This quantity is compatible with the energy flux ϵ as reported in Lindborg and Cho (2000), $\alpha^3 \approx \epsilon = 6 \times 10^{-5}$ m 2 s $^{-3}$. Standard diffusion is approached at scales larger than 2000 km. The value of the eddy diffusion coefficient is estimated by fitting the FSLE in the diffusive range with $(4 \ln r) D_E \delta^{-2}$, as shown in Boffetta et al. (2000a) by means of a dimensional argument. We find that this value is $D_E \approx 10^7$ m 2 s $^{-1}$. At small scales (100 km or less) the FSLEs tend to a plateau of level ~ 1 day $^{-1}$, suggesting an exponential separation. Notice that the initial threshold does not much affect the general behavior in the large-scale range (> 100 – 200 km), except for obvious changes in the statistical samples.

In order to appreciate the difference between the fixed-scale and fixed-time statistics, in Fig. 4 we show the dispersion rate $\lambda'(\delta)$ as defined in Eq. (2.6), to be compared to the FSLE $\lambda(\delta)$ defined in Eq. (2.5). The diffusivity $\lambda'(\delta)$ has a slope that is rather sensitive to the initial conditions and affected by a noisier statistic than the FSLE. In no way are $\lambda(\delta)$ and $\lambda'(\delta)$ expected to have necessarily the same behavior for the reasons discussed above.

Figure 5 shows global (mainly zonal) and meridional [λ_{mer} , see (2.7)] FSLEs of the balloon pairs with initial threshold 100 km. We find that the dispersion is basically isotropic up to scales of about 500 km, which is in rough agreement with the results of Morel and Larchevêque [they give a value 3 times larger, but their analysis (see their Fig. 7) does not display a well-defined cutoff]. At scales larger than 500 km, the two compo-

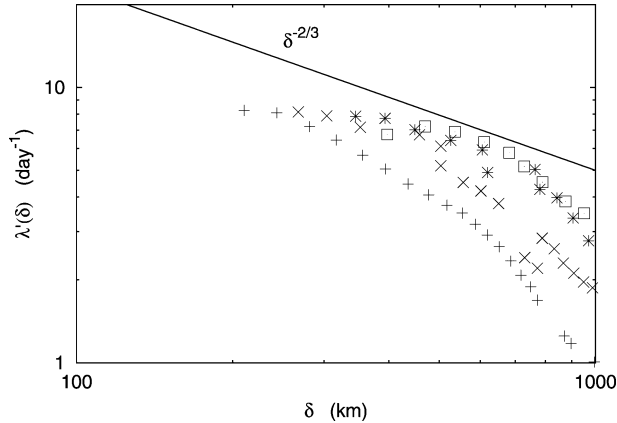


FIG. 4. Diffusivity function of the (mean) separation, as defined in Eq. (2.6). The initial thresholds are the same as in the previous figures: 25 (+), 50 (×), 100 (*), and 200 (□) km. The $\sim\delta^{-2/3}$ scaling law is plotted for comparison. The slopes are noisier and depend more sensitively on the initial conditions than the FSLE's.

nents of the FSLE decouple, and the meridional dispersion rate follows the standard diffusion law $\sim\delta^{-2}$ with a meridional eddy diffusion coefficient $D_E \sim 10^6 \text{ m}^2 \text{ s}^{-1}$.

In order to compute the FSRV, the relative velocity between balloons is approximated by the finite difference formula $(|R(t + \Delta t)| - |R(t)|)/\Delta t$, where $|R(t)|$ is the absolute value of the great circle arc between two balloons at time t , and $\Delta t = 0.04$ days is the time interval between two successive points along a trajectory. The properties of the Lagrangian relative velocity are shown in Fig. 6. The FSRV confirms the results obtained with the FSLE: between 100 and 1000 km, the behavior is $\sim\delta^{2/3}$, corresponding to the Richardson's law; asymptotic saturation sets in beyond this range (fully uncorrelated velocities).

4. Discussion and conclusions

We have revisited the dispersion properties of the EOLE Lagrangian dataset using a new approach, the finite-scale Lyapunov exponent, which is better suited to analyze scale-dependent properties than standard tools that were used, for example, by ML in a previous study of the same dataset. We were motivated by the fact that ML found results supporting a k^{-3} inertial range between 100 and 1000 km, whereas more recent studies based on aircraft data found a $k^{-5/3}$ behavior in the same range of scales. Moreover, ML did not find consistency between relative diffusivity and mean square relative velocity, the latter being compatible with a Richardson's regime (see ML's Fig. 9).

The main result of our improved analysis is that the EOLE dataset supports a $k^{-5/3}$ behavior in the range 100–1000 km, as shown by the scaling properties of FSLE in this range, indicating Richardson's superdiffusion. At distances smaller than 100 km, our results

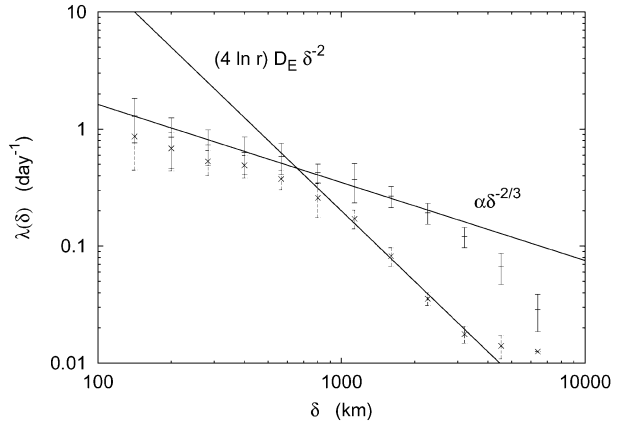


FIG. 5. FSLE of the balloon pairs, (—) describing total and (×) meridional dispersion, with initial 100-km threshold. The meridional FSLE is λ_{mer} defined in Eq. (2.7). The meridional eddy diffusion coefficient is $D_E \approx 1.5 \times 10^6 \text{ m}^2 \text{ s}^{-1}$.

suggest an exponential separation with an e -folding time of about 1 day, in rough agreement with ML. At scales larger than 1000 km, the dispersion tends to a standard diffusion before saturating at the planetary scale. Since the large-scale flow is dominated by the meandering zonal circulation, estimated diffusion coefficient is 10 times larger for total dispersion ($10^7 \text{ m}^2 \text{ s}^{-1}$) than for meridional dispersion ($10^6 \text{ m}^2 \text{ s}^{-1}$). Results coming from fixed-scale mean dispersion rates, the FSLE, and fixed-scale mean square relative velocities, the FSRV, are consistent with each other.

The physical reasons underlying a $k^{-5/3}$ spectrum are still open to debate. Possible explanations may concern 2D inverse energy cascade, gravity wave breaking with direct energy cascade, or shear (zonal) dispersion in a diffusive (meridional) field.

Our study of the EOLE experiment has shown that this still unparalleled dataset of Lagrangian trajectories in the atmosphere is in agreement with results obtained

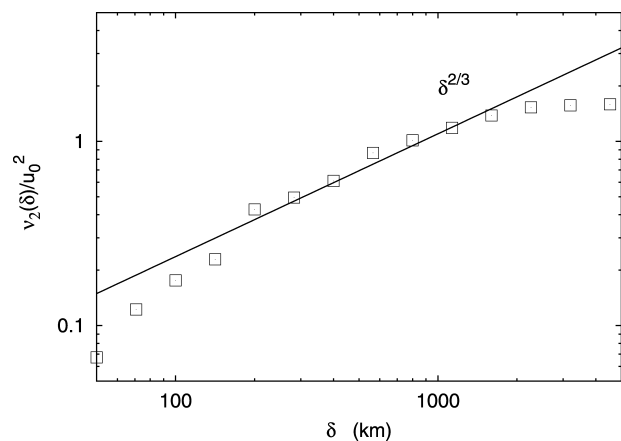


FIG. 6. FSRV [see Eq. (2.8)], of the balloon pairs for initial 50-km threshold. The reference velocity is $u_0 = 100 \text{ km h}^{-1}$. The slope $2/3$ corresponds to the Richardson's law.

from aircraft data. The challenge is now to compare these trajectories with the global wind fields produced by the recent reanalysis by operational weather centers.

Acknowledgments. We warmly thank two anonymous referees for their constructive reviews, and also, G. Boffetta, F. D'Andrea, V. Daniel, B. Joseph, A. Mazzino, and F. Vial for interesting discussions and suggestions. G.L. thanks the European Science Foundation for financial support through a TAO Exchange Grant 1999, and the LMD-ENS (Paris) for hosting him.

REFERENCES

- Artale, V., G. Boffetta, A. Celani, M. Cencini, and A. Vulpiani, 1997: Dispersion of passive tracers in closed basins: Beyond the diffusion coefficient. *Phys. Fluids*, **9**, 3162–3171.
- Aurell, E., G. Boffetta, A. Crisanti, G. Paladin, and A. Vulpiani, 1997: Predictability in the large: An extension of the concept of Lyapunov exponent. *J. Phys. A: Math. Gen.*, **30**, 1–26.
- Bacmeister, J. T., S. D. Eckermann, P. A. Newman, L. Lait, K. R. Chan, M. Lowenstein, M. H. Proffitt, and B. L. Gary, 1996: Stratospheric horizontal wavenumber spectra of winds, potential temperature, and atmospheric tracers observed by high-altitude aircraft. *J. Geophys. Res.*, **101** (D5), 9441–9470.
- Boffetta, G., A. Celani, M. Cencini, G. Lacorata, and A. Vulpiani, 2000a: Non-asymptotic properties of transport and mixing. *Chaos*, **10**, 1–9.
- , M. Cencini, S. Espa, and G. Querzoli, 2000b: Chaotic advection and relative dispersion in a convective flow. *Phys. Fluids*, **12**, 3160–3167.
- , G. Lacorata, G. Redaelli, and A. Vulpiani, 2001: Barriers to transport: A review of different techniques. *Physica D*, **159**, 58–70.
- Cho, J. Y. N., and E. Lindborg, 2001: Horizontal velocity structure functions in the upper troposphere and lower stratosphere. 1. Observations. *J. Geophys. Res.*, **106**, 10 223–10 232.
- Desbois, M., 1975: Large-scale kinetic energy spectra from Eulerian analysis of EOLE wind data. *J. Atmos. Sci.*, **32**, 1838–1847.
- Er-El, J., and R. L. Peskin, 1981: Relative diffusion of constant-level balloons in the Southern Hemisphere. *J. Atmos. Sci.*, **38**, 2264–2274.
- Fung, J. C. H., J. C. R. Hunt, N. A. Malik, and R. J. Perkins, 1992: Kinematic simulation of homogeneous turbulence by unsteady random Fourier modes. *J. Fluid Mech.*, **236**, 281–318.
- Gage, K. S., 1979: Evidence for a $k^{-5/3}$ law inertial range in mesoscale two-dimensional turbulence. *J. Atmos. Sci.*, **36**, 1950–1954.
- Gioia, G., G. Lacorata, E. P. Marques Filho, A. Mazzino, and U. Rizza, 2004: The Richardson's Law in large-eddy simulations of boundary layer flows. *Bound.-Layer Meteor.*, in press.
- Joseph, B., and B. Legras, 2002: Relation between kinematic boundaries, stirring, and barriers for the Antarctic polar vortex. *J. Atmos. Sci.*, **59**, 1198–1212.
- LaCasce, J. H., and C. Ohlmann, 2003: Relative dispersion at the surface of the Gulf of Mexico. *J. Mar. Res.*, **61**, 285–312.
- Lacorata, G., E. Aurell, and A. Vulpiani, 2001: Drifter dispersion in the Adriatic Sea: Lagrangian data and chaotic model. *Ann. Geophys.*, **19**, 121–129.
- Legras, B., and D. G. Dritschel, 1993: Vortex stripping and the generation of high vorticity gradients in two-dimensional flows. *Appl. Sci. Res.*, **51**, 445–455.
- Lichtenberg, A. J., and M. A. Lieberman, 1982: *Regular and Stochastic Motion*. Springer-Verlag, 655 pp.
- Lilly, D. K., 1983: Stratified turbulence and the mesoscale variability of the atmosphere. *J. Atmos. Sci.*, **40**, 749–761.
- Lindborg, E., and J. Y. N. Cho, 2000: Determining the cascade of passive scalar variance in the lower stratosphere. *Phys. Rev. Lett.*, **85**, 5663–5666.
- , and —, 2001: Horizontal velocity structure functions in the upper troposphere and lower stratosphere. 2. Theoretical considerations. *J. Geophys. Res.*, **106**, 10 233–10 241.
- Morel, P., and W. Bandeen, 1973: The EOLE Experiment: Early results and current objectives. *Bull. Amer. Meteor. Soc.*, **54**, 298–306.
- , and M. Desbois, 1974: Mean 200-mb circulation in the Southern Hemisphere deduced from EOLE balloon flights. *J. Atmos. Sci.*, **31**, 394–407.
- , and M. Larchevêque, 1974: Relative dispersion of constant-level balloons in the 200-mb general circulation. *J. Atmos. Sci.*, **31**, 2189–2196.
- Nastrom, G. D., and K. S. Gage, 1985: A climatology of atmospheric wavenumber spectra of wind and temperature observed by commercial aircraft. *J. Atmos. Sci.*, **42**, 950–960.
- Newell, R. E., V. Thouret, J. Y. N. Cho, P. Stoller, A. Marengo, and H. G. Smit, 1999: Ubiquity of quasi-horizontal layers in the troposphere. *Nature*, **398**, 316–319.
- Ottino, J. M., 1989: *The Kinematics of Mixing: Stretching, Chaos and Transport*. Cambridge University Press, 378 pp.
- Richardson, L. F., 1926: Atmospheric diffusion shown on a distance-neighbor graph. *Proc. Roy. Soc. London*, **A110**, 709–737.
- Taylor, G., 1921: Diffusion by continuous movement. *Proc. London Math. Soc.*, **20**, 196–212.